Digest Journal of Nanomaterials and Biostructures Vol. 14, No. 2, April - June 2019, p. 367 - 374

COMPARATIVE INVESTIGATION OF COBALT FERRITE ($CoFe_2O_4$) AND CADMIUM FERRITE ($CdFe_2O_4$) NANOPARTICLES FOR THE STRUCTURAL, OPTICAL PROPERTIES AND ANTIBACTERIAL ACTIVITY

R. ANUSA[a,*], C. RAVICHANDRAN[a], T. V. RAJENDRAN[b],
M. V. ARULARASU[c], E. K. T. SIVAKUMAR[d]
[a]*Department of Chemistry, Easwari Engineering College, Chennai 89*
[b]*Department of Chemistry, SRM Institute of Science and Technology, Ramapuram, Chennai 89*
[c]*Department of Chemistry, Presidency college, (Autonomous), Chennai 05, India*
[d]*Centre for Nano Science and Technology, Anna University, Chennai 25*

Sol-gel synthesis of cobalt ferrite ($CoFe_2O_4$) and cadmium ferrite ($CdFe_2O_4$) nanoparticles in aqueous medium has been carried out using urea. The main advantage of using urea as a by preventing particles agglomeration and act as stabilizing agent to provides long-term stability for cobalt ferrite and cadmium ferrite nanoparticles. The particles have been characterized using X-ray diffraction (XRD), high resolution scanning electron microscopy (HR-SEM), energy dispersive X-ray (EDX), UV-Visible spectra and thermogravimetric analysis (TGA). The XRD and FT-IR results confirmed the crystal structure of $CoFe_2O_4$ and $CdFe_2O_4$. The formation of $CoFe_2O_4$ and $CdFe_2O_4$ nano- and microstructures were confirmed by HR-SEM. The optical band gaps of the prepared $CoFe_2O_4$ and $CdFe_2O_4$with different preparation methods were calculated and were found to be in the range of 2.26 - 2.40 eV. The optical property test indicates that the absorption peak of the nanoparticles shifts towards short wavelength, and the blue shift phenomenon might be ascribed to the quantum effect. The traditional sol-gel approach provides an effective way to synthesize high quality semi-conductive $CoFe_2O_4$ and $CdFe_2O_4$ nanoparticles. The disk diffusion antibacterial assay of $CoFe_2O_4$ and $CdFe_2O_4$ nanoparticles was done against *E.coli*, *P.vulgarias* MTCC – 49132 (Gram negative) and *S.aureus* MRSA – 3391, S.*Aureus* – 25923 (Gram positive) bacteria.

(Received January 31, 2019; Accepted April 19, 2019)

Keywords: Cobalt ferrite, Nanoparticles, Sol-gel autocombustion, TGA, S.Aureus

1. Introduction

Ferrites with spinel structure represent the important class of magnetic materials. The combination of magnetic and catalytic properties makes ferrite useful in many technological applications. The basic electrical and magnetic properties of ferrite can be modified so as to suit the desire application. The modification in the properties of ferrite can be brought by various ways. One of the important ways of modification of properties is to use different synthetic methods by optimizing the synthesis parameters. A number of chemical routes have been used for the synthesis of ferrite nanoparticles. These methods include sol-gel [1], microemulsion [2], chemical co-precipitation[3] etc. Among these methods sol-gel method is widely used for the synthesis of nanoparticles of ferrite. The size and the properties of spinel ferrite nanoparticles can be greatly depend on pH, fuel, stirring time, speed and metal nitrates to fuel ratio etc. [4]. The most remarkable size dependent properties of magnetic material is an increase in electrical resistivity, saturation magnetization, coercivity etc.as compared to bulk material as the particle size reduces tonanoscale [5]. Ferrites are ferri magnetic oxides consisting of ferric oxide and metal oxides. On the basis of crystal structure ferrites are grouped into three classes namely hexagonal ferrite, garnet and spinel ferrite. The spinel ferrites are widely studied because of their numerous applications in several fields.

*Corresponding author: anu.mika1039@gmail.com

The spinel ferrite is having the chemical formula MFe_2O_4 (where M- is a divalent metal ions such as Co, Ni, Mn, Cd etc.) possess two sub-lattice namely tetrahedral A and octahedral B sites. The cations of different valence can accommodate in the interstitial sites of spinel ferrites bringing wide variation in the electrical and magnetic properties. The spinel ferrites are very much important magnetic materials due to their combined electrical and magnetic properties. In bulk form spinel ferrite has been investigated for their structural, electrical and magnetic properties by severalresearchers [6,7]. In the last ten years research on nano-size spinel ferrite has been considerably increased due to their superior properties and applications in new fields like magnetic drug delivery, catalyst, and sensors etc. [8]. Extensive work on structural and magnetic characterization of spinel ferrite in the form of nano-size has been done by many workers [9,10]. Among the different spinel ferrites cobalt ferrite ($CoFe_2O_4$) and cadmium ferrite ($CdFe_2O_4$) with inverse spinel structure are promising magnetic materials because of their moderate saturation magnetization, high electrical properties, high magneto-crystalline anisotropy, good mechanical properties and chemical stability[5]. In the literature synthesis and investigation of magnetic properties of spinel cobalt ferrite and cadmium ferrite nano particles have been carried out by several workers [11,12]. The large number of researchers has reported magnetic properties of cobalt ferrite nano particles with a view to understand magnetism at nano scale and their possible practical applications. However, very less attention has been paid to study the catalytic properties of cobalt ferrite and cadmium ferrite nano particles. The investigations of catalytic properties of cobalt ferrite and cadmium ferrite nano particles are important from the point of view of its use in optical and catalytic applications. The aim of the present work is to synthesize cobalt and cadmium ferrite nanoparticles by sol-gel auto-combustion method and to investigate the structural and catalytic properties. The sol-gel auto-combustion method requires low temperature and less time, produces homogenous particles of uniform size [13]. The porosity of the spinel ferrite produced by sol-gel auto-combustion method is high which leads to increases in the resistivity. In the present work, we report the structural, optical and antibacterial properties of cobalt ferrite ($CoFe_2O_4$) and cadmium ferrite ($CdFe_2O_4$) nanoparticles.

2. Experimental methods

2.1. Materials

Iron nitrate, Cobalt nitrate, Cadmium nitrate and urea purchased from Merck, were of purity 98-99%. All the chemicals used were analytical grade and used as such.

2.2. Sample preparation

All the reagents used for the synthesis of cobalt ferrite and cadmium ferrite nanoparticles were analytical grade and used as such received without further purification. The stoichiometric amounts of cobalt ferrite ($Co(No_3)_2.6H_2O$) (6.2021 g) and ferric nitrate($Fe(NO_3)_2.9H_2O$) (17.2191 g) were dissolved in deionized water under magnetic stirring. Then urea (NH_2CONH_2) (13.4347 g) was mixed in the metal nitrate solution to chelate Co^{2+} and Fe^{2+} ions in the solution. The molar ratio of urea to total moles of nitrates was maintained at 1:3.A small amount of ammonia was added drop-wise into the solution to adjust pH value to about 7 and stabilize the nitrate-urea solution. The solution was then brought to reaction temperature about 80°C and stirred for two hours. After stirring, the solution was cooled and washed by repeated decantation with water till free from nitrate ions. The product obtained were centrifuged for 20 minutes and dried overnight at 100°C. Finally the burnt powders were annealed at temperature 550^0C for 4 hrs with a heating rate of 50^0C per minute to obtain the spinel phase. The Cadmium ferrite nanoparticles were prepared by the above method using cadmium nitrate instead of cobalt nitrate and iron nitrate. The obtained powder ferrite nanoparticles were used for further characterization. (Schematic diagram represent in Scheme 1).

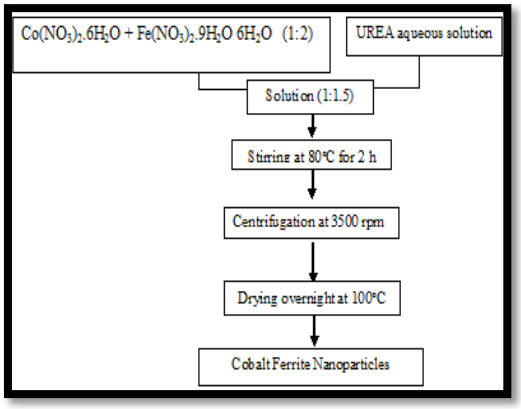

Scheme 1 Diagram of Cadmium ferrite nanoparticles preparation

2.3. Characterization

The synthesized two spinel ferrites were characterized by various techniques. The formation of spinel ferrite nanoparticles was confirmed by Fourier transform infrared (FT-IR) spectroscopy. Structure and crystallinity of synthesized nanoparticles was analysed by X-ray diffraction technique (XRD). The microstructure and particle size of the nanoparticles were determined from Scanning electron microscopy (SEM) images. The crystallinity change during heating was analysed by Thermo gravimetric analysis (TGA).

2.4. Antimicrobial Activity

In-vitro bactericidal assay was performed against both gram positive and gram negative bacterial strains *S.aureus* MRSA – 3391, S.*Aureus* – 25923, like *E.coli*, *P.vulgarias* MTCC - 49132. These strains were sub cultured from the pure culture obtained from King Institute of preservative medicine and research (Chennai) and characterized. Antimicrobial activity was analyzed using the Kirby-Bauer disk diffusion method, using the prepared $CoFe_2O_4$ and $CdFe_2O_4$, along with a positive control and blank disk was used as a negative control. The cultures were incubated at $\pm$37 ^oC for 24 hours and the zone of inhibition was observed.

3. Result and discussions

3.1. Fourier-Transform Infrared (FT-IR) spectroscopy

The FT-IR spectra recorded for the cobalt and cadmium ferrite nanoparticles and shown in Fig. 1. The corresponding stretching vibrations of –OH groups obtained at 3368-3371 cm^{-1}. The peaks at 1598-1618 cm^{-1} indicates flexible vibrations of –OH groups caused by adsorbed water or humidity[14]. It is suggested that the surface of the samples contain active –OH groups. At low wave number, the peaks in the range of 828 to 764 cm^{-1}corresponds to metal-oxygen (Fe-O) stretching vibrations and it is characteristic peak of the spinel structure of cobalt and cadmium ferrites.

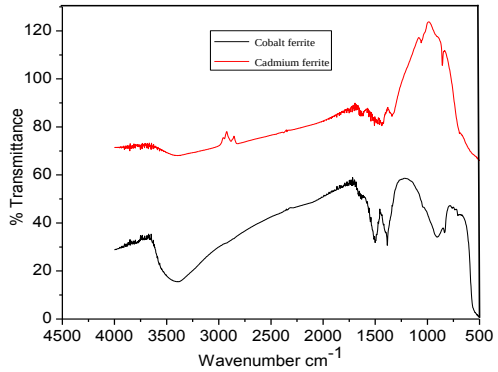

Fig. 1. FT-IR spectra of cobalt and cadmium ferrite nanoparticles.

3.2. X-ray diffraction studies

The lattice parameters, structure and crystallite size of the synthesized cobalt and cadmium ferrite were recognized by powder XRD pattern. The XRD pattern of synthesized cobalt and cadmium ferrite was exposed in Fig. 2(a) and (b). The average crystallite size of synthesized samples was calculated by using Scherrer formula $d = 0.89\lambda/\beta\cos\theta$ [15] where d is the average crystallite size, λ, the X-ray wavelength (0.154 nm), θ, Bragg's angle, and β the peak position[30]. The $CoFe_2O_4$ nanoparticles indicated cubic final structure (JCPDS card No. 22-1086) and $CdFe_2O_4$ nanoparticles indicated cubic final structure (JCPDS card No. 22-1063). From the XRD results all synthesized cobalt and cadmium ferrites were pure structure without impurities and their crystallite values are seemed in single digits. The average crystalline size of cobalt and cadmium ferrite nanoparticle, were calculated as 35 nm and 52 nm respectively.

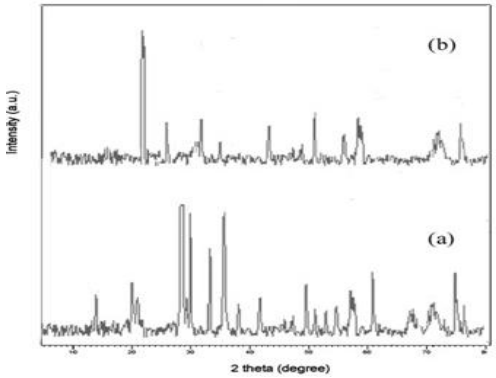

Fig. 2. XRD patterns of a) cobalt; b) cadmium ferrite nanoparticles.

3.3. Scanning Electron Microscopy (SEM)

The SEM images of cobalt and cadmium ferrite nanoparticles are shown in Fig. 3 (a) and (b) respectively and it reveals that sample exhibit a compact arrangement of homogeneous nanoparticles with spherical in shape. The results illustrated that cobalt and cadmium ferrites have small size and good dispersion rate. The FESEM images of prepared samples are easy to see a combination and collision of small spherical. Some particles are slightly aggregated but not truly. Actual morphology of each ferrite expresses different dimension due to growth and nucleation process due to the preparation method.

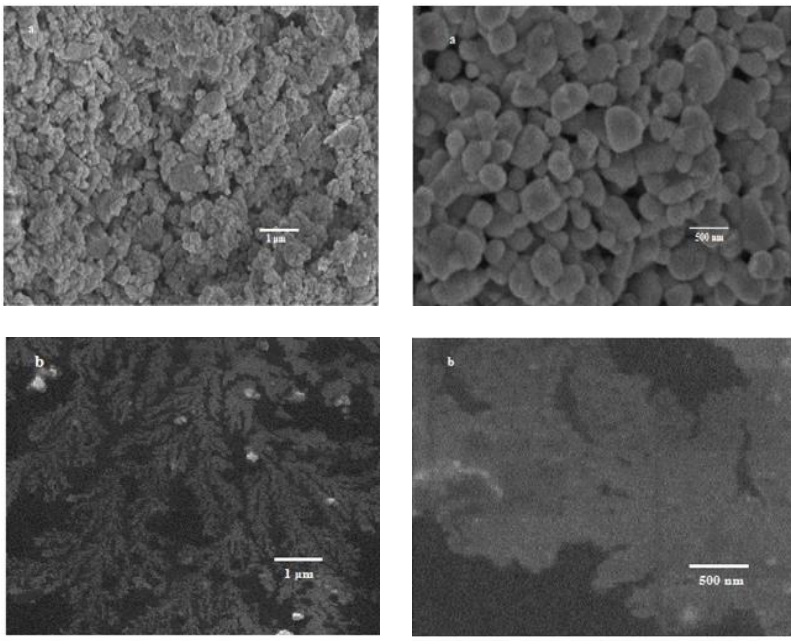

Fig. 3 SEM images of a) cobalt; b) cadmium ferrite nanoparticles.

3.4. TGA analysis

Thermo gravimetric analysis of synthesized cobalt and cadmium ferrite nanoparticles are shown in Fig. 4. The synthesized ferrite nanoparticles were heated from 100^{o}C to 900^{o}C under flowing N_2 and changes in mass losses are recorded. The weight loss in the temperature range of 200^{o}C to 300^{o}C which may due to evaporation of hydroxyl groups adsorbed on the surface of nanoparticles during synthesis. The last broadened exothermic peak at 780^{o}C and 800^{o}C with small weight loss could be considered as a solid reaction attributed to the gradual formation of cobalt and cadmium ferrite [16,17]. After 850^{o}C, no further distinguishable weight loss was detected, indicating that all organic constituents were eliminated.

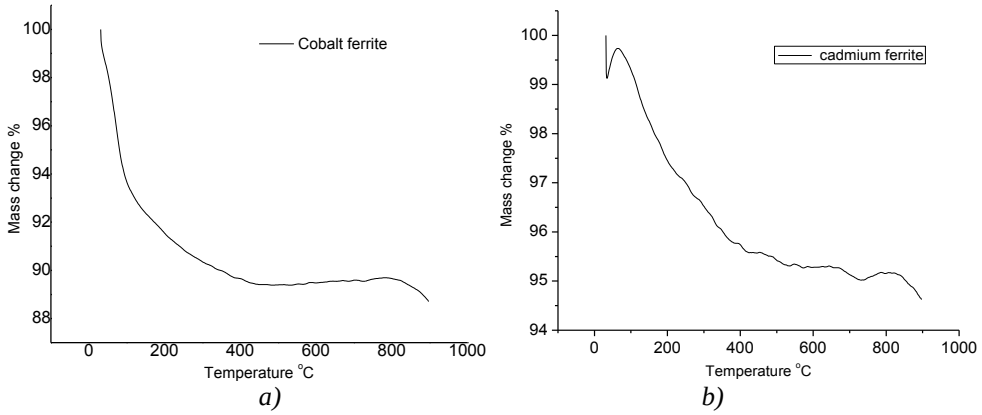

Fig. 4. TGA analysis of
a) cobalt ferrite nanoparticles; b)cadmium ferrite nanoparticles.

3.5. UV-Vis Spectroscopy

The optical properties are very significant to select the materials for its distinct applications. Accordingly, this study the band gap of the cobalt and cadmium ferrite nanoparticles were estimated. The band gap of the materials plays a crucial role in decide the photocatalytic

activity which participates in arbitrate the electron – hole recombination rate [18,19]. Fig. 5 shows the UV–vis. absorption spectrum of the synthesized sample. Fig. 5 (a-b) represents the optical absorption spectra of sample A and B obtained of single absorption peak at 457 nm (2.26 eV) and 485 nm (2.40 eV) respectively. The excitation peak only depends on the short axis on the particles and the $CoFe_2O_4$ and $CdFe_2O_4$ nanoparticles grown large the long axis grows beyond the confinement region this is the reason for the blue shift of the excitation peak. The result indicates that the absorption band has slightly shifted in the visible region. On account of the desired crystalline nature, the sample shows a good absorption of visible light. It is notable that, tetrahedral and octahedral sites are occupied by M^{2+} and Fe^{3+} cations, respectively in the normal spinel type compound $CoFe_2O_4$ and $CdFe_2O_4$. The optical band gaps (E_g) of cobalt and cadmium ferrite samples were calculate by $(\alpha h\nu)^2$ vs $h\nu$ [20], where α,h and ν are the absorption coefficient, Plank's constant and photo frequency respectively. It can be undoubtedly attribute the aqueous synthesis of $CoFe_2O_4$ nanoparticles band gap of 2.26 eV due to decrees particle size on increasing crystallinity of the sample.

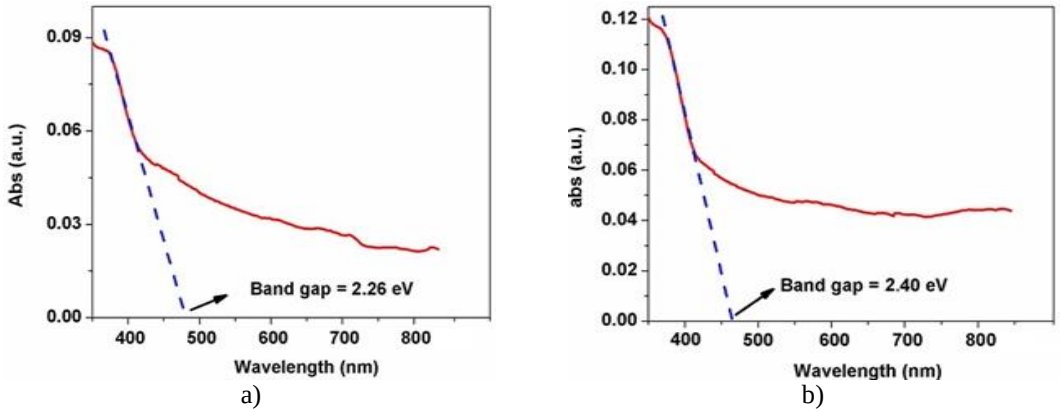

Fig. 5. UV Visible spectra of a) cobalt and b) cadmium ferrite nanoparticles.

3.6. Antibacterial activity

The antibacterial activity of the synthesized spinel $CoFe_2O_4$ and $CdFe_2O_4$ nanoparticles was tested against *E.coli*, *P.vulgarias* MTCC – 49132 (Gram negative) and *S.aureus* MRSA – 3391, S.*Aureus* – 25923 (Gram positive) bacteria using disc diffusion method. Fig. 6 represents the photographs of the antibacterial tests and results obtained are summarized in Table 1.

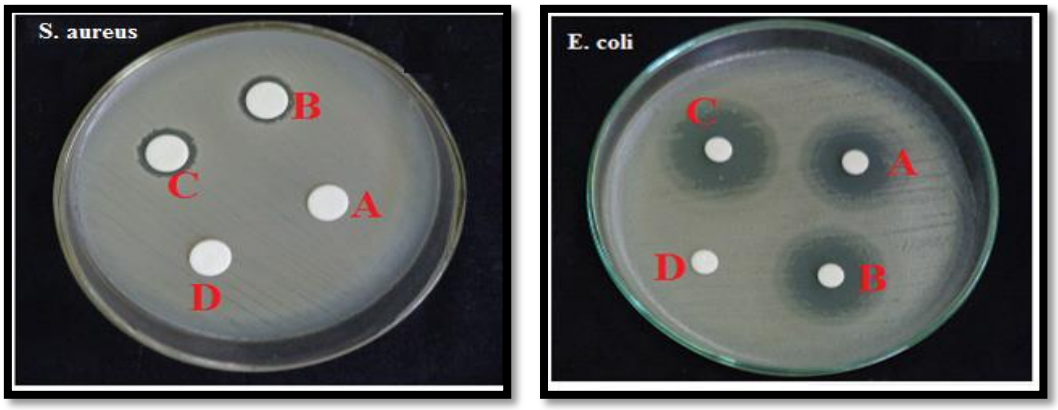

Fig. 6. Antibacterial studies of cobalt and cadmium ferrite nanoparticles.

The presence of an inhibition zone clearly indicates the antibacterial effect of the $CoFe_2O_4$ and $CdFe_2O_4$ nanoparticles. The $CoFe_2O_4$ and $CdFe_2O_4$ prepared by sol-gel method sample show much higher activity against Gram negative than against Gram positive. The higher zone of inhibition efficiency in the case of gram negative bacteria as compared to gram positive ones was reported earlier. The antibacterial activity is greatly depends on the size of nanoparticles and also difference in the cell wall [14,21]. This may be correlated to the difference in the cell wall structure of *E.coli*, *P.vulgarias* MTCC – 49132 (gram negative) and *S.aureus* MRSA – 3391, S.*Aureus* – 25923 (gram positive). E.coli and S. aureus bacteria have similar internal, but very different external structure. The gram positive bacteria have a peptidoglycan layer that layer contains lipoteichoic and trichoic acids. The gram negative bacteria have thin peptidoglycan layer and an outer membrane that contains proteins, phospholipids and lipoplysaccharide. These allow outcome on that the bacteria photoinactivation rate is control not only by cell wall thickness but also by envelop resistance of outer membrane to the reactive oxygen species produced at the photocatalytic surface and the morphology of cell.

Table 1. Zones of inhibition (mm) values against the Gram negative for Fe_2O_4 nanoparticles.

No.	A $CoFe_2O_4$ 8µg/Disc (8µg/µl)	B $CdFe_2O_4$ 8µg/Disc (8µg/µl)	C Standard 1µg/Disc (1µg/1µl)	D Sterile disc
1	14 mm	12 mm	16 mm	0 mm

Table 2. Zones of inhibition (mm) values against the Gram positive for Fe_2O_4 nanoparticles.

No.	A $CoFe_2O_4$ 8µg/Disc (8µg/µl)	B $CdFe_2O_4$ 8µg/Disc (8µg/µl)	C Standard 1µg/Disc (1µg/1µl)	D Sterile disc
1	0 mm	1 mm	1 mm	0 mm

This result suggests that the aqueous synthesized ferriate can be used as an productive application of antibacterial material. The enhanced antibacterial activity together with the large surface area of the ferriate to physical and chemical properties of the nanoparticles. This is explaining a large number of nanoparticles were greatly dispersed per unit area of the ferriate surfaces, thus, maximizing antibacterial activity. Nanoparticles are mostly attached on ferriate surfaces which assure even dispersion, as unsupported nanoparticles tend to agglomerate and thus break into their final properties.

4. Conclusions

Nanocrystalline transition metal doped Fe_2O_4 powders were successfully fabricated using the sol-gel-auto combustion method. Compared with other ferrite ($CoFe_2O_4$ and $CdFe_2O_4$ nanoparticles), the antibacterial activity of $CdFe_2O_4$ has showed superior killing rate because of its spherical shape and crystallinity. The optical properties of these ferrite extremely based on the morphology and the nature of the transition metal. The entire characterization results were assisted to identify the shape, size and chemical combination and band gap of the synthesized spinel ferrite. Work is currently in progress to use nanosized fabricated materials for water purification and the removal of pollutants from wastewater.

References

[1] A. V. Kadu, S. V. Jagtap, G. N. Chaudhari, Current Applied Physics **9**, 1246 (2009).
[2] H. Nathani, S. Gubbala, R. D. K. Misra, Materials Science and Engineering **121**, 126 (2005).
[3] M. R. Anantharaman, S. Jagatheesan, K. A. Malini, S. Sindhu, A. Narayanasamy, C. N. Chinnasamy, J. P. Jacobs, S. Reijne, K. Seshan, R. H. H. Smits, H. H. Brongersma, Journal of Magnetism and Magnetic Materials **189**, 83 (1998).
[4] B. Rudraji, H. Tangsali Satish, K. Keluskar Ganpat, E. Naik, S. Budkuley, S. D. Shenoy, P. A. Joy, M. R. Anantharaman, Journal ofMagnetism and Magnetic Materials **269**, 217 (2004).
[5] V. Mukta, B. Limaye Shashi, K. Singh Sadgopal Date, V. Deepti Kothari Raghavendra Reddy, Ajay Gupta, Vasant Sathe, RamJane Choudhary, Sulabha K. Kulkarni, J. Phys. Chem. **B113**, 9070 (2009).
[6] I. C. Nlebedimn, N. Ranvah, P. I. Williams, Y. Melikhov, J. E. Snyder, A. J. Moses, D. Jiles, C. J Magn. Magn. Mater **322**, 1929 (2010).
[7] M. V. Arularasu, R. sundaram, Sensing and Bio-Sensing Research **11**, 20 (2016).
[8] R. Sasmita Mohapatra Smruti, Rout SwatilekhaMaiti Tapas K. Maiti, Asit B. Panda, J. Mater. Chem. **21**, 9185 (2011).
[9] K. Maaz, S. Karim, A. Mumtaz, S. K. Hasanain, J. Liu, J. L. Duan, J Magn. Magn.Mater. **321**, 1838 (2009).
[10] Y. Ichiyanagi, M. Kubota, S. Moritake, Y. Kanazawa, T. Yamada, T. Uehashi, J. Magn. Magn. Mater. **310**, 2378 (2007).
[11] Lawrence Kumar, Manoranjan Kar. J. Magn. Magn. Mater. **323**, 2042 (2011).
[12] N. M. Deraz, J. Analyt. Appl. Pyro. **88**, 103 (2010).
[13] G. S. Pozan, M. Isleyen, S. Gokcen, Applied Catalysis B: Environmental **140**, 537 (2013).
[14] M. V. Arularasu, J. Devakumar, T.V. Rajendran, Polyhedran, **156**, 279 (2018).
[15] M. V. Arularasu, J. Devakumar, R.Sundaram, J. Supercond. Nov. Magn. **9** (31), 2983 (2018).
[16] R. C. Merkle, Nanotechnology **11**, 89 (2000).
[17] M. H. Habibi, A. H. Habibi, Journal of Thermal Analysis and Calorimetry **113**, 843 (2013).
[18] M. V. Arularasu, M. Anbarasu, S. Poovaragan, R. Sundaram, K. Kanimozhi, C. Maria Magdalane, K. Kaviyarasu, F. T. Thema, M. Mazza, Journal of Nanoscience and Nanotechnology**18**, 3511 (2018).
[19] C. Maria Magdalane, K. Kaviyarasu, A. Raja, M. V. Arularasu, Genene T. Mola, Abdulgalim B. Isaev, Naif Abdullah Al-Dhabi, Mariadhas Valan Arasu, B. Jeyaraj, J. Kennedy, M. Maaza, J. of Photochemistry and Photobiology B: Biology **185**, 275 (2018).
[20] M. V. Arularasu, R. Sundaram, C. Maria Magdalane, K. Kanimozhi, K. Kaviyarasu, F. T. Thema, D. Letsholathebe, M. Maaza, Journal of Nanostructure **7**, 47 (2017).
[21] S. I. Shanthi, S. Poovaragan, M. V. Arularasu, S. Nithya, R. Sundaram, C. Maria Magdalene, K. Kaviyarasu, M. Maaza, J. Nanosci. Nanotechnol. **18,** 5441 (2018).